CODEN IEJMAT *Internet Electronic Journal of Molecular Design* **2007**, *6*, 000–000 ISSN 1538–6414
BioChem Press http://www.biochempress.com

Inter*net* Electronic Journal of Molecular Design

October 2007, Volume 6, Number 10, Pages 320–330

Editor: Ovidiu Ivanciuc

3D–QSAR CoMFA Study on Human Glutaminyl Cyclase Inhibitors

Munuganti Ravi Shashi Nayana,[1] Yadavalli Nataraja Sekhar,[1] Nunna Siva Kumari,[1] and Shaik Mahmood [1]

[1] Bioinformatics Division, Environmental Microbiology Lab, Department of Botany, Osmania University, Hyderabad 500007, Andhra Pradesh, India

Received: May 9, 2007; Revised: July 4, 2007; Accepted: August 30, 2007; Published: October 31, 2007

Citation of the article:
M. R. S. Nayana, Y. N. Sekhar, N. S. Kumari, and SK. Mahmood, 3D–QSAR CoMFA Study on Human Glutaminyl Cyclase Inhibitors, *Internet Electron. J. Mol. Des.* **2007**, *6*, 320–330, http://www.biochempress.com.

Copyright © 2007 BioChem Press

Inter*net* Electronic Journal of Molecular Design

BioChem Press
http://www.biochempress.com

3D–QSAR CoMFA Study on Human Glutaminyl Cyclase Inhibitors

Munuganti Ravi Shashi Nayana,[1,*] Yadavalli Nataraja Sekhar,[1] Nunna Siva Kumari,[1] and Shaik Mahmood [1,*]

[1] Bioinformatics Division, Environmental Microbiology Lab, Department of Botany, Osmania University, Hyderabad 500007, Andhra Pradesh, India

Received: May 9, 2007; Revised: July 4, 2007; Accepted: August 30, 2007; Published: October 31, 2007

Internet Electron. J. Mol. Des. **2007**, *6* (10), 320–330

Abstract

Motivation. Glutaminyl cyclase (QC), besides its crucial role in hormone maturation and its pathophysiological involvement in Alzheimer's disease, is a new potential drug target. To understand the structural requirements of QC ligands and to design new ligands against human glutaminyl cyclase with enhanced inhibitory potency we performed a 3D–QSAR (quantitative structure–activity relationships) study with comparative molecular field analysis (CoMFA) for a dataset of 50 imidazole derivatives which are inhibitors of human glutaminyl cyclase.

Method. Comparative molecular field analysis (CoMFA) QSAR models were computed with Sybyl 6.7v.

Results. The 3D–QSAR model has very good statistics, namely leave–one–out (LOO) cross–validated correlation coefficient q^2 = 0.647, non–cross–validated correlation coefficient r^2 = 0.917, and the predicted correlation coefficient r^2_{pred} = 0.652.

Conclusions. Based on the high values for q^2 and r^2 we are confident that the 3D–QSAR model gives good predictions that may be used to design better QC inhibitors. The CoMFA model reveals the most significant correlation of steric and electrostatic fields with biological activities. The information derived from this study provides a tool for guiding further structural modification to obtain more potent inhibitors of QC.

Keywords. Human glutaminyl cyclase; quantitative structure–activity relationships; 3D–QSAR; comparative molecular field analysis; CoMFA; imidazole derivatives.

Abbreviations and notations

QC, glutaminyl cyclase	QSAR, quantitative structure–activity relationships
CoMFA, comparative molecular field analysis	PLS, partial least squares
LOO, leave–one–out	

1 INTRODUCTION

Glutaminyl cyclases (QC) [1] (E.C.2.3.2.5) are acyltransfarases that are abundant in mammalian neuro endocrine tissues, such as hypothalamus and pituitary [2,3]. Some peptide hormones, such as thyrotropin releasing hormone (TRH) and gonadotropin releasing hormone (GnRH), require the

* Correspondence author; phone: +919985795735; E–mail: rs_nayana@rediffmail.com; phone: +919849602498; E–mail: skmahmood@osmania.ac.in.

pGlu on the N–terminus for their biological activity [4,5]. Interestingly, the formation of pGlu is related to the formation of several plaque–forming peptides, such as amyloid–β (Aβ) peptides and collagen–like Alzheimer's amyloid plaque component, which plays a pivotal role in Alzheimer's disease (AD) [6,7]. Peptides containing N–terminal pGlu [*e.g.*, $pGlu^3$–Aβ (3–40) and $pGlu^3$–Aβ (3–42/43)], are major fractions of the Aβ peptides within the core of neurotic plaques [8,9]. The N–terminal pGlu could enhance the hydrophobicity, proteolytic stability, and neurotoxicity of these peptides [10,11], probably causing an accumulation of pGlu–Aβ peptides in several senile plaques and thus accelerating the progression of neurodegenerative disorders. Hence, besides the crucial role in hormone maturation, human QC might be involved in the pathophysiological process of AD, evoking its qualification as a new potential drug target [12].

Quantitative structure–activity relationships (QSAR) models establish statistical relationships between the biological activity exerted by a series of compounds and a set of parameters determined from their structures (structural descriptors). The factors contributing to the biological activity can be understood through use of different physicochemical descriptors in the generation of QSAR models [13]. Two components are essential for QSAR models; the first component is the computation of the structural descriptors from the three–dimensional molecular structure. Various geometrical, quantum, or molecular field descriptors were proposed in recent years to substitute the Hansch substituent constants. The second component in a 3D–QSAR model is an explicit mathematical structure activity relationship established between a dependent variable (biological activity) and a set of independent variables (3D structural descriptors); the mathematical 3D–QSAR equations can be computed with the help of a large number of statistical models, such as multilinear regression, partial least squares (PLS), or artificial neural networks. Some 3D–QSAR models also contain a third component, a graphical representation of the three–dimensional information relative to the ligand–receptor interactions encoded into the structure–activity equation [14]. An important component of all QSAR models is a proper validation and evaluation of the prediction power. The modeling competition CoEPrA (comparative evaluation of prediction algorithms) was specially devised to compare QSAR models based on blind predictions [15].

Since its introduction in 1988, comparative molecular field analysis (CoMFA) [16] has emerged as one of the most powerful tools in ligand based drug design strategies [17]. The CoMFA methodology assumes that a suitable sampling of steric and electrostatic fields around a set of aligned molecules provides all the information necessary for understanding their biological properties [18,19]. The present study is aimed to gain insights into the steric and the electrostatic properties of these compounds, their influence on the activity and to derive predictive 3D–QSAR models for design and prediction of the activities of new derivatives for this class of inhibitors.

2 MATERIALS AND METHODS

2.1 QSAR Dataset

The in vitro biological activity data reported as K_i for inhibition of human QC by the imidazole derivatives was taken from the published work of Buchholz *et al*. [12] and used for the current study (Table 1). The reported K_i values were converted into the corresponding pK_i values.

Three–dimensional structure building and all modeling were performed using the Sybyl program package, version 6.7 [20] on a Silicon Graphics Fuel workstation. Energy minimization was performed using the Tripos force field [21] and the Gasteiger–Huckel charge with a distance–dependant dielectric and Powell conjugate gradient algorithm with convergence criterion of 0.005 kcal/mol. Partial atomic charges were calculated using the semiempirical program MOPAC 6.0 with the AM1 Hamiltonian.

2.2 Alignment

In the present study the MOPAC geometry optimized structures were aligned on the template 28B, which is the most active molecule among the given set. All the molecules were aligned by the ALIGN DATABASE command available in SYBYL using maximum substructure. It adjusts the geometry of the molecules such that its steric and electrostatic fields match the fields of the template molecule.

2.3 CoMFA

The steric and electrostatic CoMFA potential fields were calculated at each lattice intersection of a regularly spaced grid of 2.0 Å. The grid box dimensions were determined automatically in such a way that region boundaries were extended beyond 4 Å in each direction from coordinates of each molecule. The van dar Waals potentials and coulombic terms were calculated using the Tripos force field. An sp^3 hybridized carbon atom with +1 charge served as probe atom to calculate steric and electrostatic fields. The steric and electrostatic contributions were truncated to +30.0 kcal/mol.

2.4 Partial Least Square (PLS) Analysis

The CoMFA descriptors were used as independent variables, and pK_i values as dependant variables in partial least square regression analysis. The minimum sigma (column filtering) was set to 2.0 kcal/mol to improve the signal–to–noise ratio. The predictive correlation coefficient (r^2_{pred}) based on the test molecules, is computed with the formula r^2_{pred} = (SD–PRES)/SD, where SD is the sum of the squared deviations between the biological activities of the test set and mean activities of training set molecules and PRESS is the sum of squared deviation between predicted and actual activity for every molecule in test set.

Table 1. Structures, K_i and pK_i Values of Compounds **1–50**

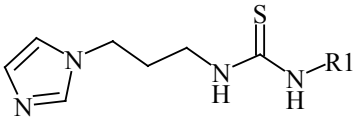

A1–19

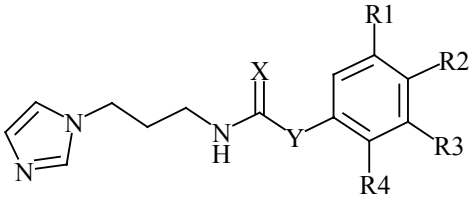

B20–28

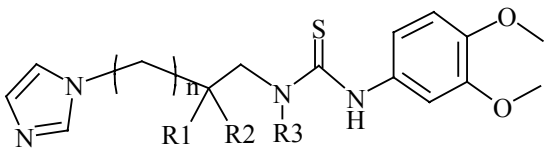

C29–33

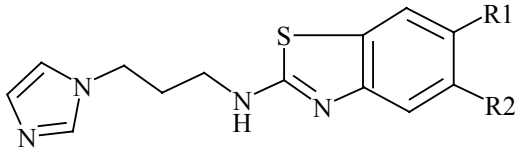

D34–37

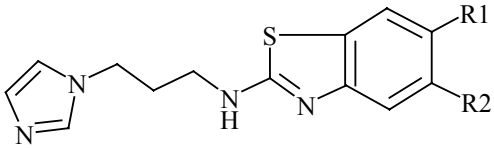

E38–50

Comp.	Label in [12]	R_1	R_2	R_3	R_4	X	Y	n	K_i (μM)	pK_i
1A	**26**	CH_3	–	–	–	–	–	–	13.02	4.885
2A	**27**	$(CH_2)_3CH_3$	–	–	–	–	–	–	4.65	5.332
3A	**28**	$C(CH_3)_3$	–	–	–	–	–	–	14.72	4.832
4A	**29**	$CH(CH_3)_2$	–	–	–	–	–	–	11.30	4.947
5A	**30**		–	–	–	–	–	–	3.66	5.436
6A	**31**		–	–	–	–	–	–	4.70	5.328
7A	**32**	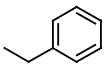	–	–	–	–	–	–	5.67	5.246
8A	**33**		–	–	–	–	–	–	4.48	5.349
9A	**34**	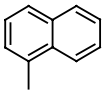	–	–	–	–	–	–	2.79	5.554
10A	**35**	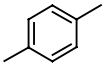	–	–	–	–	–	–	2.14	5.669
11A	**36**	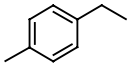	–	–	–	–	–	–	2.78	5.556
12A	**37**	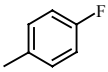	–	–	–	–	–	–	4.73	5.325
13A	**38**	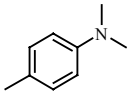	–	–	–	–	–	–	2.03	5.692

Table 1. (Continued)

Comp.	Label in [12]	R_1	R_2	R_3	R_4	X	Y	n	K_i (μM)	pK_i
14A	**39**	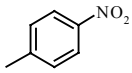	–	–	–	–	–	–	2.68	5.572
15A	**40**	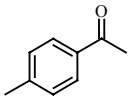	–	–	–	–	–	–	1.79	5.747
16A	**41**	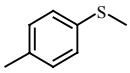	–	–	–	–	–	–	1.66	5.780
17A	**42**	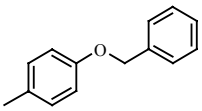	–	–	–	–	–	–	0.97	6.013
18A	**43**	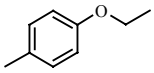	–	–	–	–	–	–	0.89	6.051
19A	**44**	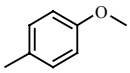	–	–	–	–	–	–	0.70	6.155
20B	**45**	H	–OCH_2O–		H	S	NH	–	5.66	5.247
21B	**46**	OMe	H	H	H	S	NH	–	1.86	5.730
22B	**47**	H	OMe	OMe	H	S	$NHCH_2$	–	1.55	5.809
23B	**48**	H	–OCH_2CH_2O–		H	S	NH	–	1.12	5.951
24B	**49**	OMe	H	OMe	H	S	NH	–	0.75	6.125
25B	**50**	H	OMe	H	OMe	S	NH	–	0.56	6.252
26B	**51**	H	OMe	OMe	H	O	NH	–	0.49	6.309
27B	**52**	OMe	OMe	OMe	H	S	NH	–	0.34	6.468
28B	**53**	H	OMe	OMe	H	S	NH	–	0.06	7.222
29C	**55**	H	H	H	–	–	–	2	0.55	6.259
30C(*R*)	**56**	Me	H	H	–	–	–	1	0.34	6.469
31C(*S*)	**57**	H	Me	H	–	–	–	1	0.76	6.119
32C	**58**	–$(CH_2)_2$–		H	–	–	–	1	2.33	5.633
33C	**59**	H	H	Me	–	–	–	1	4.83	5.317
34D	**66**	H	H	–	–	–	–	–	3.73	5.428
35D	**67**	Cl	H	–	–	–	–	–	3.35	5.475
36D	**68**	OMe	H	–	–	–	–	–	1.57	5.804
37D	**69**	OMe	OMe	–	–	–	–	–	2.00	5.699
38E	**70**	OMe	OMe	H	H	–	–	–	0.39	6.409
39E(*R*)	**71**	H	H	Me	H	–	–	–	7.34	5.134
40E(*S*)	**72**	H	H	H	Me	–	–	–	3.51	5.455
41E	**73**	H	H	H	Ph	–	–	–	4.48	5.349
42E	**74**	OMe	H	–$(CH_2)_2$–		–	–	–	0.40	6.398
43E	**75**	Cl	H	–$(CH_2)_3$–		–	–	–	4.88	5.311
44E	**76**	Cl	H	–$(CH_2)_4$–		–	–	–	7.33	5.135
45E	**77**	OMe	H	–$(CH_2)_5$–		–	–	–	2.22	5.654
46E	**81**	OMe	OMe	–$(CH_2)_2$–		–	–	–	0.09	7.046
47	**85**	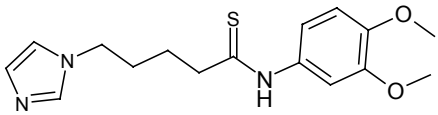				–	–	–	0.99	6.004

Table 1. (Continued)

Comp.	Label in [12]	R_1	X	Y	n	K_i (μM)	pK_i
48	**1**	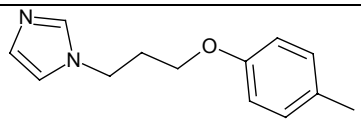	–	–	–	7.70	5.113
49	**2**	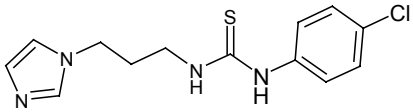	–	–	–	0.03	5.906
50	**3**	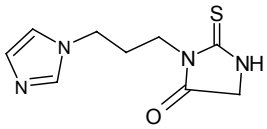	–	–	–	0.7	6.115

3 RESULTS AND DISCUSSION

A total of 50 compounds were partitioned into a training set of 33 and a test set of 17 compounds at random. Bias given to both structural and biological diversity in both the sets. Table 2 lists experimental activities, predicted activities and residual values of the training set and test set by CoMFA model. This study gave the LOO cross–validated coefficient q^2 values of 0.647 and non–cross validated correlation coefficient, r^2, 0.917 for CoMFA (Table 3). All the aligned molecules are shown in Figure 1, and Figure 2 shows the correlation between the experimental and predicted pK_i values for CoMFA.

Table 2. Experimental and Calculated pK_i Values of Compounds from the Training and Test Sets

Comp. [a]	Exp. pK_i	Calc. pK_i	Residual
1A*	4.885	5.221	–0.336
2A	5.332	5.394	–0.062
3A	4.832	5.227	–0.395
4A	4.947	4.963	–0.016
5A*	5.436	5.012	0.424
6A	5.328	5.436	–0.108
7A	5.246	5.165	0.081
8A	5.349	5.334	0.015
9A	5.554	5.478	0.076
10A	5.669	5.775	–0.106
11A*	5.556	5.618	–0.062
12A*	5.325	5.800	–0.475
13A	5.692	5.810	–0.118
14A	5.572	5.789	–0.217
15A	5.747	5.384	0.363
16A	5.780	5.618	0.162
17A	6.013	6.070	–0.057
18A	6.051	6.221	–0.170
19A	6.155	6.155	0.141
20B*	5.247	5.926	–0.679
21B*	5.730	5.048	0.682
22B	5.809	5.444	0.365
23B*	5.951	5.750	0.201
24B*	6.125	5.598	0.527

Table 2. (Continued)

Comp. [a]	Exp. pK_i	Calc. pK_i	Residual
25B	6.252	6.249	0.003
26B	6.309	5.810	0.499
27B	6.468	6.685	–0.217
28B	7.222	6.254	0.968
29C*	6.259	5.829	0.430
30C(*R*)	6.469	6.567	–0.098
31C(*S*)	6.119	6.270	–0.151
32C*	5.633	6.036	–0.403
33C	5.317	6.060	–0.743
34D	5.428	5.355	0.073
35D	5.475	5.580	–0.105
36D*	5.804	5.613	0.191
37D	5.699	5.925	–0.226
38E*	6.409	5.859	0.55
39E(*R*)	5.134	5.290	–0.156
40E(*S*)*	5.455	5.253	0.202
41E	5.349	5.163	0.186
42E	6.398	6.477	–0.079
43E	5.311	5.603	–0.292
44E	5.135	5.036	0.099
45E*	5.654	5.103	0.551
46E	7.046	6.433	0.613
47*	6.004	5.737	0.267
48*	5.113	5.285	–0.172
49	5.906	5.592	0.314
50*	6.115	5.698	0.417

[a] Compounds labeled with * are included in the test set

Table 3. CoMFA PLS Result Summary

q^2	r^2	r^2_{pred}	r^2_{LFO}	n	F value	SEE	Steric	Electrostatic
0.647	0.917	0.652	0.662	5	59.524	0.177	0.498	0.502

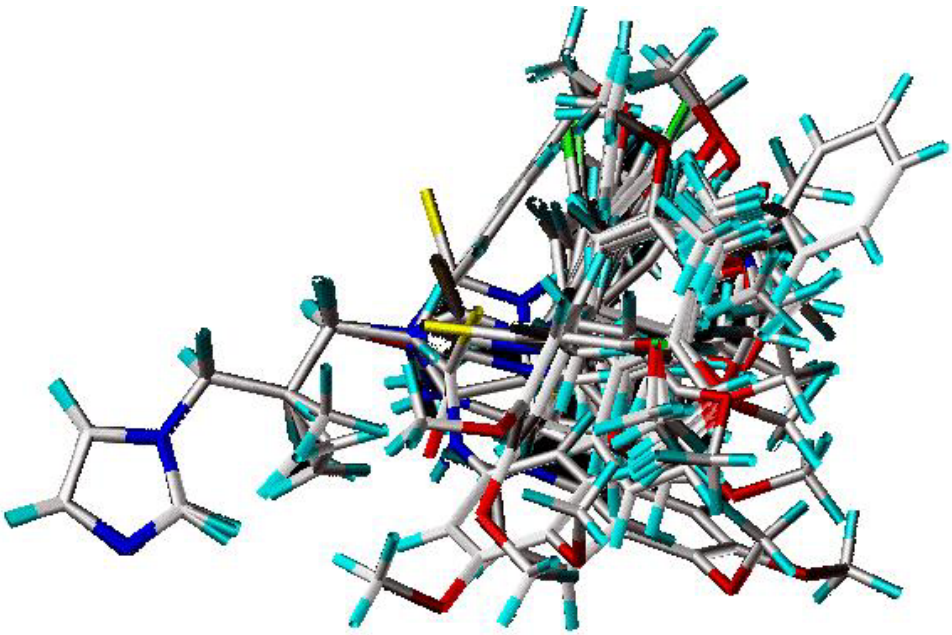

Figure 1. Alignment of all molecules used for molecular field generation

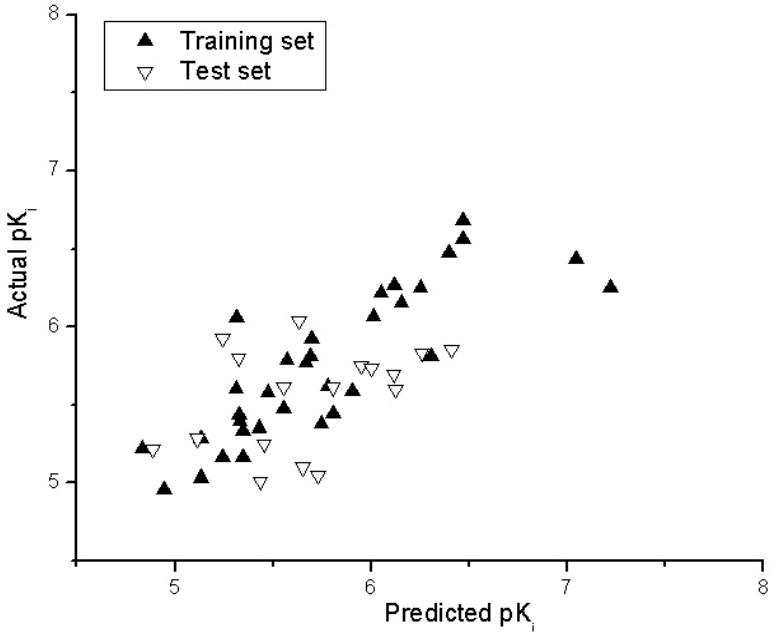

Figure 2. Plot of actual versus predicted pK_i values for the CoMFA model

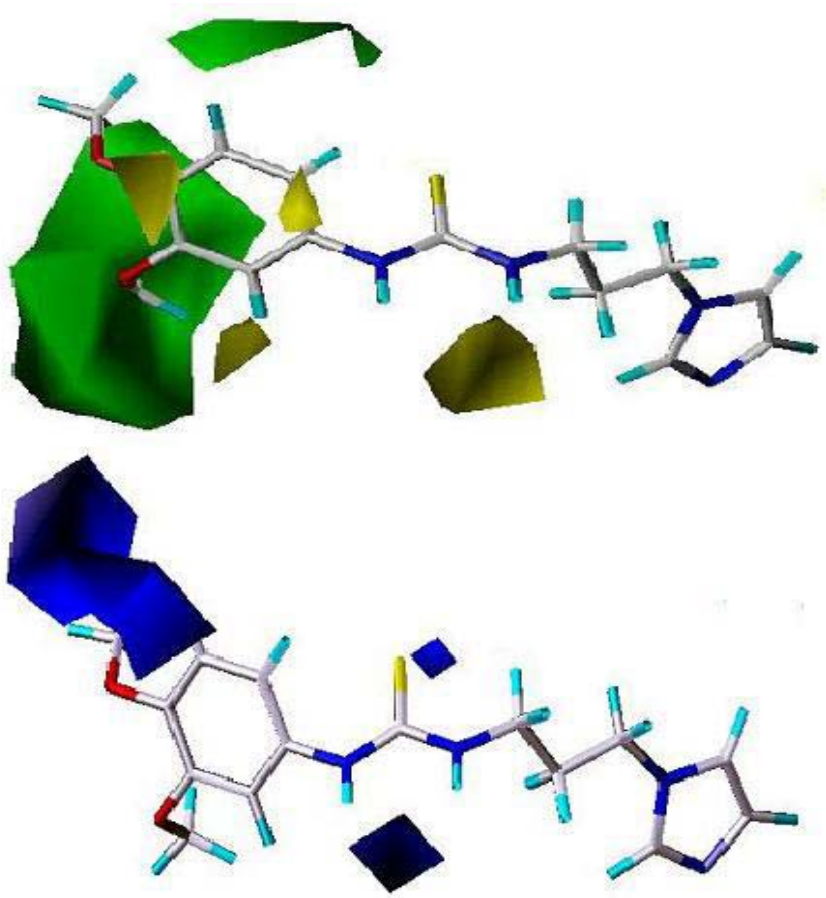

Figure 3. Steric and electrostatic contour maps for **28B**, a highly active human QC inhibitor. Sterically favored areas in green; sterically disfavored areas in yellow. Positive potential areas in blue, and negative potential favored areas in red (no red contours in the plot).

3.1 CoMFA Contour Analysis

The steric and electrostatic contour maps for human QC inhibitory model are displayed in the Figure 3. The steric plot shows three small sized yellow contours around a phenyl ring, disfavoring bulky groups in these regions. Substitution of cycloalkyl group at R_3 and R_4 (compounds with **E** scaffold) position shows detrimental effect on inhibitory potency. For example, compounds **43E–48** have poor activities. Compounds **1A–6A**, with their bulky aliphatic chains, cycloalkyl ring and norbornyl residues also exhibit poor activity. Another big yellow contour near the Nitrogen atom also disfavors substitution of methyl group in this region. Compound **33C**, substituted with methyl at the R_3 position, has poor activity. Other compounds with a **C** scaffold have shown better activity, except for **32C**, which has cycloalkyl group. In the displayed plot, one medium sized green contour runs above the phenyl ring, while another, large sized green contour runs around it, indicating that substitution of a methoxy group on the phenyl ring has led to a great increase of inhibitor potency. Therefore, compounds **24B**, **26B**, **27B**, **28B**, **30C**, **38E**, **42E** and **46E** exhibit good activity.

The electrostatic plot shows two small blue contours supporting the thio–amide group for better activity. This explains why compound **26B** shows reduced activity compared to **28B**. The substitution of sulfur, a weaker electronegative atom than oxygen enhances the inhibitory potency. Any change in this region leads to a decrease in inhibitory potency, as may be observed in similar compounds, mentioned in Table 1. In the same plot, there is a big blue contour around the phenyl ring, favoring negative inductive effect (–I) groups, namely NO_2, NR and OR. This pattern can be observed in compounds **13A**, **14A**, **24B**, **27B**, **29C–31C**, **38E** and **46E**. We also found that compounds having strong –I groups like NO_2, NR exhibit less activity than weak –I groups such as OR.

4 CONCLUSIONS

In the current study, we have successfully established the ligand–based 3D QSAR CoMFA model on 50 imidazole derivatives, reported as QC inhibitors. This model has good statistical results in terms of q^2 and r^2 values and showed a great predictivity of the test set, in the external validation, without visible outliers. The model gave q^2 and r^2 values of 0.647 and 0.917. The CoMFA results suggest that steric interactions (49.8%) as well as electrostatic interactions (50.2%) contribute to the activities of inhibitors. Using a test of 17 ligands, we were able to demonstrate that the model is also predictive for new compounds.

The effect of steric and electrostatic fields around aligned molecules was clarified by analyzing CoMFA contour maps. The analysis of CoMFA contour maps suggested that substitution of aliphatic chains and cycloalkyl rings at R_1 (**A** scaffold) and R_3, R_4 (**E** scaffold) positions will cause reduction in the activity. CoMFA contour maps favor the substitution of Oxygen with Sulfur at thio–amide region. Substitution of methoxy group at *meta* and *para* position on phenyl ring largely

contributes to a great increase in the inhibitory activity. This comparative analysis of contour maps is expected to be of an aid in the design of compounds with an enhanced inhibitory activity and better selectivity to glutaminyl cyclase protein.

Acknowledgment

The Authors are thankful to the UGC Government of India for financial support. We are thankful to the management of PGRRCDE, Osmania University for providing the software facility and for continuous support to carry out this work.

Supplementary Material

An sd file containing the structures and activities of 50 imidazole derivatives is available as supplementary material.

5 REFERENCES

[1] K. Richter, E. Kawashima, R. Egger, and G. Kreil, Biosynthesis of thyrotropin releasing hormone in the skin of Xenopus laevis: partial sequence of the precursor deduced from cloned cDNA. *EMBO. J.* **1984**, *3*, 617–621.

[2] A. Oberg, J.M. Ruysschaert, M. Azarkan, N. Smolders, S. Zerhouni, R.Wintjens, A. Amrani, and Y. Looze, Papaya glutamine cyclase, a plant enzyme highly resistant to proteolysis, adopts an all–beta conformation. *Eur. J. Biochem*. **1998**, *258*, 214–222.

[3] P. A. Sykes, S. J. Watson, J. S. Temple, and R. C. Jr. Bateman, Evidence for tissue–specific forms of glutaminyl cyclase, *FEBS Lett*.**1999**, *455*, 159–161.

[4] A. C. Awade, P. Cleuziat, T. Gonzales, and J. Robert–Baudouy, Pyrrolidone carboxyl peptidase (Pcp): An enzyme that removes pyroglutamic acid (pGlu) from pGlu–peptides and pGlu–proteins. *Proteins*. **1994**, *20*, 34–51.

[5] J. S. Garavelli, The RESID database of protein structure modifications: 200 update, *Nucleic Acids Res*. **2000**, *563*, 191–196.

[6] C. Morgan, M. Colombres, M. T. Nunez, and N. C. Inestrosa, Structure and function of amyloid in Alzheimer's disease. *Prog. Neurobiol*. **2004**, *74*, 323–349.

[7] T. Hashimoto, T. Wakabayashi, A. Watanabe, H. Kowa, R. Hosoda, A. Nakamura, I. Kanazawa, T. Arai, K. Takio, and D. M. A. Mann. CLAC: a novel Alzheimer amyloid plaque component derived from a transmembrane precursor, CLAC–P/collagen type XXV. *EMBO J*. **2002**, *21*, 1524–1534.

[8] T. C. Saido, T. Iwatsubo, D. M. Mann, H. Shimada, Y. Ihara, and S. Kawashima, Involvement of pyroglutamine endolysis followed by pyroglutamate formation in the pathogenesis of triplet repeat/pyroglutamine–expansion deseases. *Neuron* **1995**, *14*, 1524–1534.

[9] Y. M. Kuo, M. R. Emmerling, A. S. Woods, R. J. Cotter, and A. E. Roher, *Biochem. Biophys. Res. Commun*. **1997**, *237*, 188–191.

[10] C. Russo, E. Violani, S. Salis, V. Venezia, V. Dolcini, G. Damonte, U. Benatti, C. D'Arrigo, and P. Carlo, *J. Neurochem*. **2002**, *82*, 1480–1489.

[11] Y. Harigaya, T. C. Saido, C. B. Eckman, C. M. Prada, M. Shoji, and S. G. Younkin, Isolation, Chemical Characterization, and Quantitation of Aβ 3–Pyroglutamyl Peptide from Neuritic Plaques and Vascular Amyloid Deposits. *Biochem. Biophys. Res. Commun*. **2000**, *276*, 422–427.

[12] M. Buchholz, U. Heiser, S. Schilling, A. J. Neistroj, K. Zunkel, and H. U. Demuth, The first potent inhibitors for Human Glutaminyl Cyclase: Synthesis ans structure–Activity relationship. *J. Med. Chem*. **2006**, *49*, 664–677.

[13] S. M. Vadlamudi and V. M. Kulkarni, 3D–QSAR of Protein Tyrosine Phosphatase 1B Inhibitors by Genetic Function Approximation. *Internet Electron. J. Mol. Des*. **2004**, *3*, 586–609.

[14] O. Ivanciuc, 3D QSAR Models. In: QSPR/QSAR Studies by Molecular Descriptors. Ed.: M. V. Diudea. Nova Science, Huntington, N.Y., **2001**, pp. 233–280.

[15] http://www.coepra.org

[16] R. D. Cramer III, D. E. Patterson, and J. D. Bunce, Comparative molecular field analysis (CoMFA). 1. Effect of shape on binding of steroids to carrier proteins. *J. Am. Chem. Soc*. **1988**, *110*, 5959–5967.

[17] G. R. Desiraju, B. Gopalakrishnan, R. K. Jetti, A. Nagaraju, J. D. Raveendra, A. Sharma, and R. Thilagavathi, Computer–Aided Design of Selective COX–2 Inhibitors: Comparative Molecular Field Analysis, Comparative Molecular Similarity Indices Analysis, and Docking Studies of Some 1,2–Diarylimidazole Derivatives. *J. Med.*

Chem. **2002**, *45*, 4847–4857.

[18] S. K. Singh, N. Dessalew, and P. V. Bharatam, 3D–QSAR CoMFA study on indenopyrazole derivatives as cyclin dependent kinase 4 (CDK4) and cyclin dependent kinase 2 (CDK2) inhibitors. *Eur*. *J*. *Med*. *Chem*. **2006**, *41*, 1310–1319

[19] R. Thilagavathi and A. K. Chakraborti, Importance of Alignment in Developing 3–D QSAR Models of 1,5–Diaryl Pyrazoles for the Prediction of COX–2 Inhibitory Activity. *Internet Electron*. *J*. *Mol*. *Des*. **2005**, *4*, 603–612.

[20] SYBYL, version 6.7; Tripos Associates: St. Louis, MO, **2000**

[21] M. Clark, R. D. Cramer III, and N. Van Opdenbosch, Validation of the general purpose Tripos 5.2 force field, *J*. *Comput*. *Chem*, **1989**, *10*, 982–1012.

Biographies

Munuganti Ravi Shashi Nayana is Research Scholar working for Ph.D degree from Osmania University. His area of interest is Computational Drug Designing.

Yadavalli Nataraja Sekhar is Post Graduate in M. Tech. majoring in Industrial Biotechnology, Anna University, Tamilnadu.

Nunna Siva Kumari is Post Graduate in Biochemistry, Andhra University. Her area of interest is proteomics.

Shaik Mahmood M.Sc., Ph.D. Assistant Professor and Joint Co–ordinator for Bioinformatics, Osmania University. Areas of interest are bacterial production of biopolymers and bioinformatics.